Triple-shell symmetry in α-(Al,Si)-Mn

H. A. Fowler
Center for Applied Mathematics, National Bureau of Standards, Gaithersburg, Maryland 20899

B. Mozer
Institute for Materials Science and Engineering, National Bureau of Standards, Gaithersburg, Maryland 20899

J. Sims
Center for Applied Mathematics, National Bureau of Standards, Gaithersburg, Maryland 20899
(Received 14 September 1987)

We describe three-dimensional graphics modeling experiments executed on a calligraphic system. Utilizing precise data from neutron diffraction, a triple icosahedral shell has been identified in the α-(Al,Si)-Mn phase. These triple shells are centered in the unit cell; the $Pm\bar{3}$ structure is completed by double shells on the cube corners. The triple shell can also be viewed as a composite of twelve coordination icosahedra around the maganese sites on the second (MacKay) shell.

INTRODUCTION

The detailed geometry of atomic positions in alloys containing icosahedral structures has been a continuing subject of curiosity and speculation. Guyot, Audier, and collaborators[1,2] and Elser and Henley[3-5] have studied the direct-space geometry of the α phase of (Al,Si)-Mn and have compared it with icosahedral phases of the ternary and of Al-Mn, using face matching Amman rhombohedra with various schemes of decoration. A new basis of experimental data is provided by the recent work of Cahn, Gratias, and Mozer,[6] which compares the α-cubic and icosahedral phases of (Al,Si)-Mn, using Patterson diagrams. Here we develop the α-cubic data in full graphical detail, to illustrate the nature of the local cluster formations.

This family of aluminum-manganese alloy phases exhibits the common structural feature[1,2,6-8] of icosahedral shells based upon a hollow center surrounded by 12 aluminum atoms, within a second shell of 12 manganese atoms situated concentric to the first, with 30 aluminum sites distributed on a near sphere between the manganese sites. The second shell of 42 atoms is usually described as a MacKay icosahedron, although, as we shall see, its form departs from the flat icosahedral planar faces which were hypothesized in MacKay's original plan.[9] These double shells, which seem to possess considerable structural stability in the rapid-cooling processes by which these alloys are formed, are found with common orientation of their icosahedral axis systems; however, in different alloy phases they are found to be distributed on a variety of lattice forms. A recent paper evaluating the fine-grain contributions to cohesive energy by manganese and aluminum atoms[10] bases a local-effective-density principle upon the patterns of icosahedral neighbors, of which these shells are detailed examples.

EXPERIMENTAL METHOD

The sample of Al (62 wt. %), Mn (28 wt. %), Si (10 wt. %) was carefully prepared by rapid solidification to assure complete homogenization, and then powdered. The finely sieved powder was annealed at 500 °C for 30 h in an alert atmosphere, to produce the α crystalline phase, which was then checked by x-ray diffraction.

The neutron diffraction experiments were performed on the high-resolution five-counter powder diffractometer at the National Bureau of Standards Reactor, with neutrons of wavelength 1.548 Å. The data was collected in the angular range 5°–120°, using horizontal beam collimators for the in-pile monochromatic beam, and diffracted beams of 10, 20, and 10 min, respectively. The sample was placed in a vanadium container which does not produce any peaks in the diffraction pattern.

DIFFRACTION ANALYSIS

In the measured diffraction pattern small peaks of aluminum, coming from precipitated aluminum in the alloy, were observed and subtracted from the data. The remaining pattern consisted of only a single phase, as determined from our refinement.

The refinement was performed using the Rietveld method[11] adapted to the five-counter diffractometer and modified to include background parameters.[12] The peak profiles in all cases were well described by a Gaussian function. In the final refinements all structural, lattice, and profile parameters were allowed to vary simultaneously, except the occupation of silicon and aluminum atoms. We assumed that the silicon atoms were randomly distributed on aluminum sites, as did Cooper and Robinson.[13] (Planned future refinements will attempt to define the occupancy of the silicon on the aluminum

sites.) The formal refinements yielded a weighted R factor in excellent agreement with the expected value, which is based upon the quality of our data as determined by the counting statistics.

GRAPHICS METHOD

To provide a direct-space model of the α phase, as a focus for the comparison of theory and experiment, we have depicted the full three-dimensional (3D) unit-cell structure in a calligraphic reconstruction. The simulation forces a reconciliation of site-symmetry details in the model. We gain a thorough visual perception of many details of spacing and symmetry which are not visible in the numerical data of the motif alone.

The instrument used is an Evans and Sutherland (E&S) PS300 graphics system, serving as a work station ahead of a VAX 11/785 computer. The geometric operations required to replicate the motif may be written as simple instructions, in the PASCAL-like language of the PS300 system. Rotations, translations, and scalings are one-line commands; reflections and inversions can be expressed as 3×3 matrices. Large composite geometric structures are described by tree-form programs; to adapt for very large trees with many levels, we have developed programs for E&S-to-FORTRAN conversion, and for fast binary file handling which lead to compatibility with the fast scanning cycle of the interpretation-and-display routines.

The procedure followed in the examples below has been to start with the motif vectors as determined from diffraction (a set of distinguishable vector positions within the unit cell); to generate replications of this set by the point-group geometric operations, while adding geometric details interactively; then to generate still larger replications using appropriate translation operators of the space group. By doing this, we reconstruct the full detail of the unit cell from its irreducible representation (in the form of the motif), while meeting the constraints imposed by direct-space packing.

TRIPLE-SHELL STRUCTURE

The data resulting from the diffraction refinement have provided precise confirmation of the lattice structure of this phase, which had been proposed earlier by Cooper and Robinson.[13] The comparative site positions in the cubic unit cell are shown in the first two blocks of Table I. There are two distinct sites for manganese atoms, and nine for aluminum. The silicon is understood to be substitutional for aluminum, and experiments do not as yet distinguish between the sites of these two atom types.

Utilizing the successive operations of three-fold rotation about (111) axis, inversion through the cell center, and reflection in y-z, z-x, x-y planes we construct a full set of sites in the unit cell, then connect these by appropriate line segments to illustrate the concentric-shell structure. This is suggested in Figs. 1(a) and 1(b). The positioning of these shells in the space-group structure is suggested by Fig. 2. The complete set of available sites is described by a packing which places triple shells around the center of each unit cell, and double shells around each cube corner.

We note that the second and third shells differ from McKay's original plan, which called for regular triangular icosahedral faces on these shells. Since the manganese corners are depressed towards the center, the second shell is nearly spherical. This shell is illustrated as a packing of spheres in Fig. 5 of Ref. 4. (To reduce visual clutter, we have omitted bonds between aluminum sites; the manganese sites are on the fivefold vertices, and the aluminum sites on the corners between, creating a tessellated ball as shown.) This arrangement permits the third shell to assume the form of a rhombic triacontahedron (30 rhombus faces), which is truncated along the threefold axes. Besides the triangular faces on threefold axes, it has elongated-hexagon faces normal to the twofold axes of the icosahedral system; six of these faces are shared between adjacent unit cells.

The structure of the large third shell incorporates the

TABLE I. Icosahedral triple shell—centered in the unit cell.

	α-(Al,Si)-Mn $Pm\bar{3}$ symmetry							α-(Al,Si)-Fe $Pm\bar{3}$ symmetry		
	Cooper and Robinson x-ray diffraction			Mozer and Cahn Neutron diffraction				Cooper (cell I) x-ray diffraction (numbering corresponds with Cooper and Robinson)		
	x	y	z	x	y	z		x	y	z
Mn(1)	0.3271	0.2006	0.0000	0.328 76	0.197 54	0.000 00	Fe(1)	0.3243	0.1981	0.0000
Mn(2)	0.1797	0.3085	0.5000	0.177 94	0.307 08	0.500 00	Fe(2)	0.1757	0.3019	0.5000
Al(1)	0.3638	0.0000	0.0000	0.367 18	0.000 00	0.000 00		0.3777	0.0000	0.0000
Al(2)	0.1216	0.5000	0.5000	0.129 18	0.500 00	0.500 00		0.1223	0.5000	0.5000
Al(4)	0.1636	0.0997	0.0000	0.164 65	0.101 34	0.000 00		0.1651	0.1006	0.0000
Al(5)	0.3342	0.3990	0.5000	0.336 51	0.401 13	0.500 00		0.3349	0.3994	0.5000
Al(8)	0.1185	0.1892	0.2980	0.117 53	0.187 50	0.299 34		0.1146	0.1872	0.3003
Al(9)	0.3897	0.3127	0.1955	0.390 99	0.314 21	0.197 30		0.3834	0.3128	0.1997
Al(3)	0.2897	0.0000	0.5000	0.289 95	0.000 00	0.500 00		0.2990	0.0000	0.5000
Al(6)	0.3319	0.4037	0.0000	0.329 14	0.401 06	0.000 00		0.3266	0.4030	0.0000
Al(7)	0.1205	0.1175	0.5000	0.122 96	0.119 27	0.500 00		0.1275	0.1170	0.5000

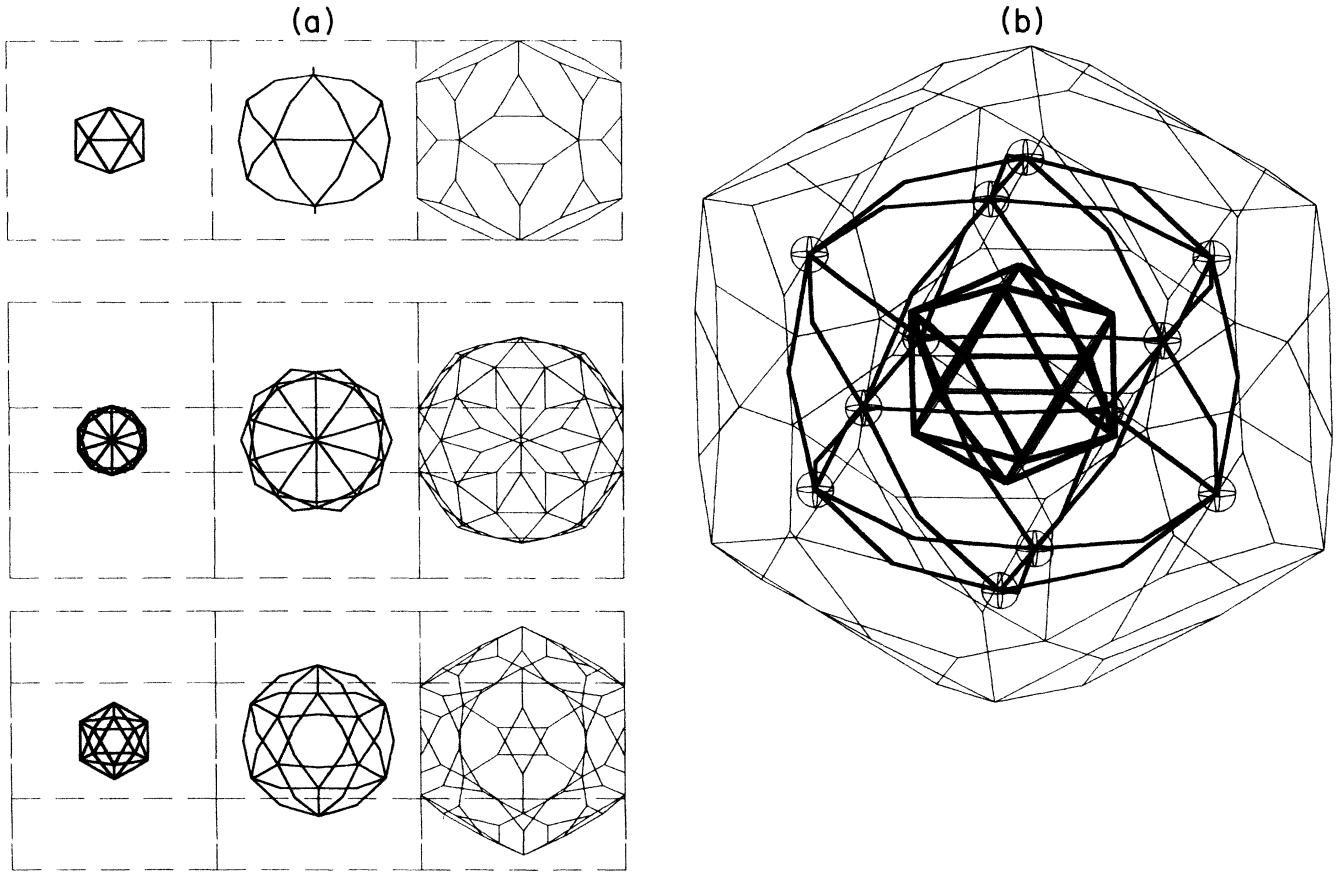

FIG. 1. (a) First, second, and third shells in α phase, centered in unit cell: (001)-axis view, threefold-axis view, pseudo fivefold-axis view. In the second shell, aluminum-to-aluminum bonds are omitted. (All figures are shown in orthographic projection.) (b) Triple-shell configuration around center of unit cell, with manganese positions indicated by small spheres.

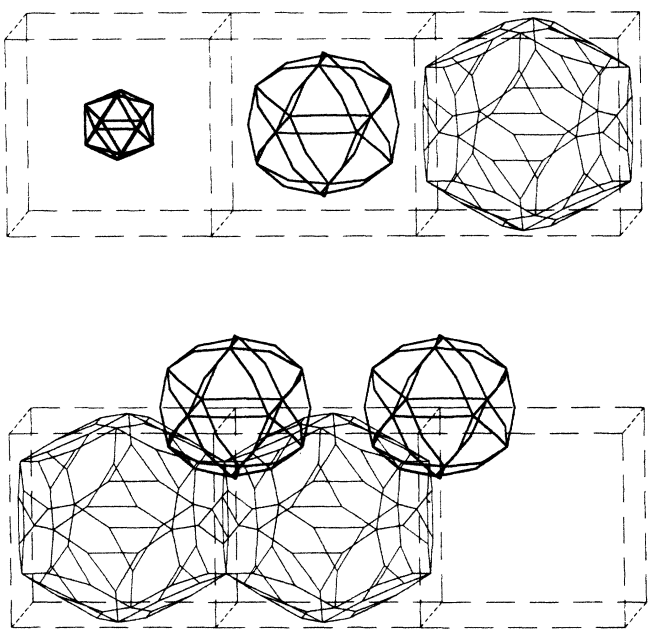

FIG. 2. Individual shells within unit cubes, triple and double shells in the center and/or corner $Pm\bar{3}$ packing, $a = 1.268$ nm.

sites labeled Al(3), Al(6), Al(7), and Al(9). At the outset, we were ignorant of its geometry; Cooper and Robinson had apparently been unaware of its high symmetry. We commenced by illustrating the packing which occurs around the [111] axis, in order to study the bonding between MacKay double shells which had been hypothesized by Guyot and Audier[1,2] and by Mozer, Cahn, Gratias, and Shechtman.[14,15] The motif structure following threefold rotation about [111] is shown in Fig. 3.

In Figs. 3(a) and 3(b), the center of the unit cell is at lower left, the corner at upper right. Outlines of the central first shell [replications of Al(4)] and second shell [sites Al(1), Al(8), and Mn(1)], also of the corner first shell [site Al(5)] and corner second shell [Al(2), Al(9), and Mn(2)] are heavily emphasized. Mn positions are indicated by large atom spheres.

Near the center plane we see a detached almost-planar ring of nine Al(3), Al(6), and Al(7) sites which are emphasized by small atom spheres. In Fig. 3(c), which is projected along the (111) axis, we see that the Al(3) sites are at a larger radial distance from the axis than the Al(6) and Al(7), on the corners. The dashed lines in these diagrams illustrate an approximate Penrose-Amman rhombohedron formed by drawing an icosahedral fivefold symmetry axis from the center through Al(4) to Mn(1), and

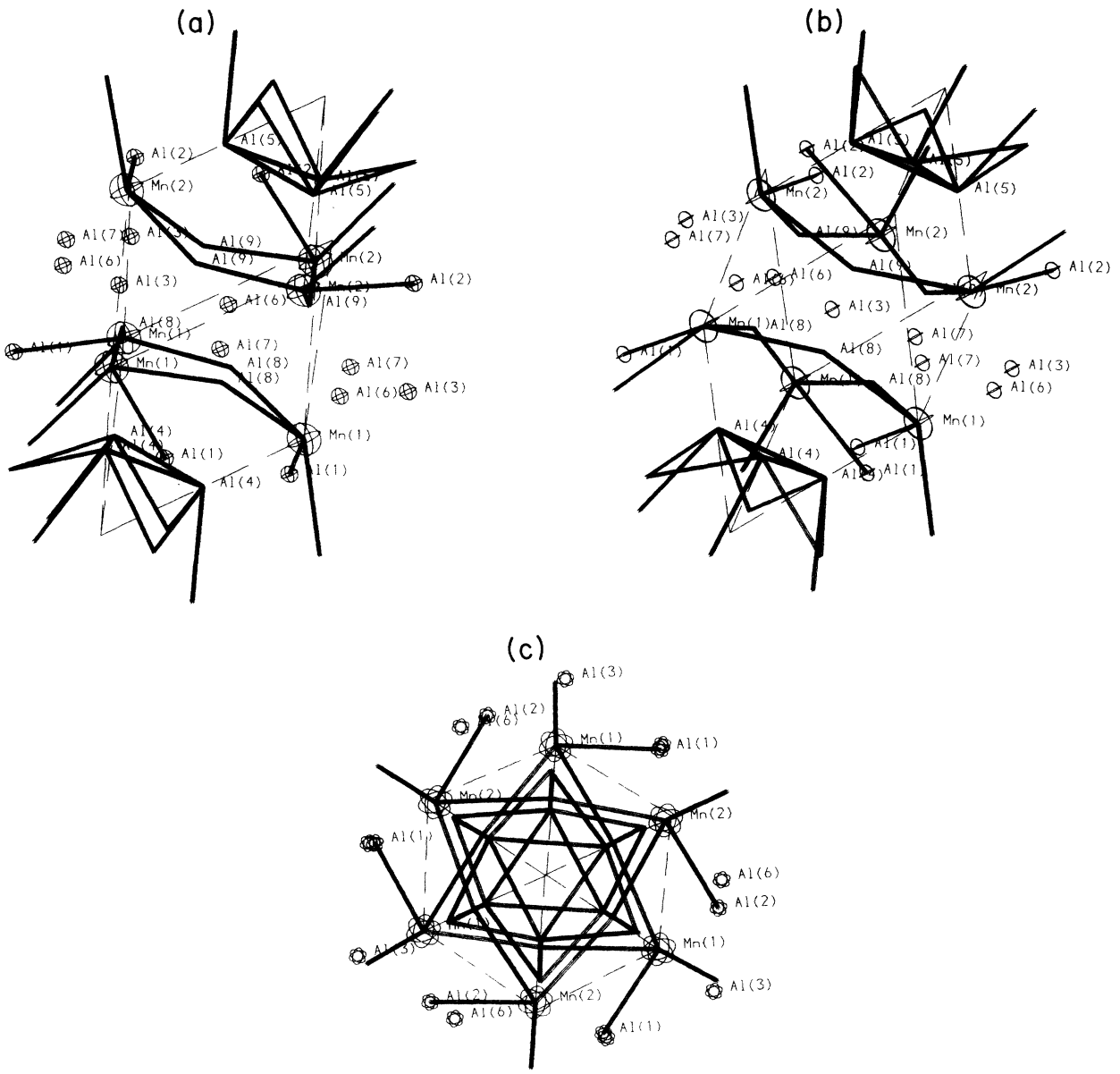

FIG. 3. (a) Motif following threefold rotation about [111]. (b) Same, rotated. (c) Same, [111]-axis view.

completing these rhombus faces, which "miss" the Mn(2) position slightly at their outer corners, where they do not quite meet the radii from the corner through Al(5) and Mn(2) sites (the misfit is comparable to that shown in Ref. 1, Fig. 10).

However, the Al(3) position lies precisely on an extension of the fivefold axis through Al(4) and Mn(1); the resulting radii are in the ratio 1:2:3 to within 2%. The Al(3) position also falls on a threefold axis when viewed from the corner as origin (this axis is normal to the center of a triangle face); thus the Al(3) site is not symmetrically positioned with respect to the two separate classes of icosahedral centers.

Guyot, Audier, and Lequette[1] illustrate the positioning of Mn(1) and Mn(2) sites, which we have suggested, in their Figs. 2(a) and 2(b). We point out that in addition to their octahedron of six manganese, we have positioned the three Al(9)'s in a small triangular shared face, and located nine sites on the ring of aluminums which surrounds each octahedron. Thus there now appears to be a large number of closely spaced sites involved in this bonding between double (MacKay) icosahedral shells.

If the remaining point-group operations (inversion, base-plane reflections) are then applied to the set Al(3), Al(6), Al(7), and Al(9), we obtain the completed third shell, which is seen in different views in Figs. 4, 5, and 6. Here we have connected the Al(3) sites to all of their neighbors within the unit cell by heavy bonds, which are found to align closely with the icosahedral fivefold directions of the interior shells.

This treatment reveals the following details of the third shell.

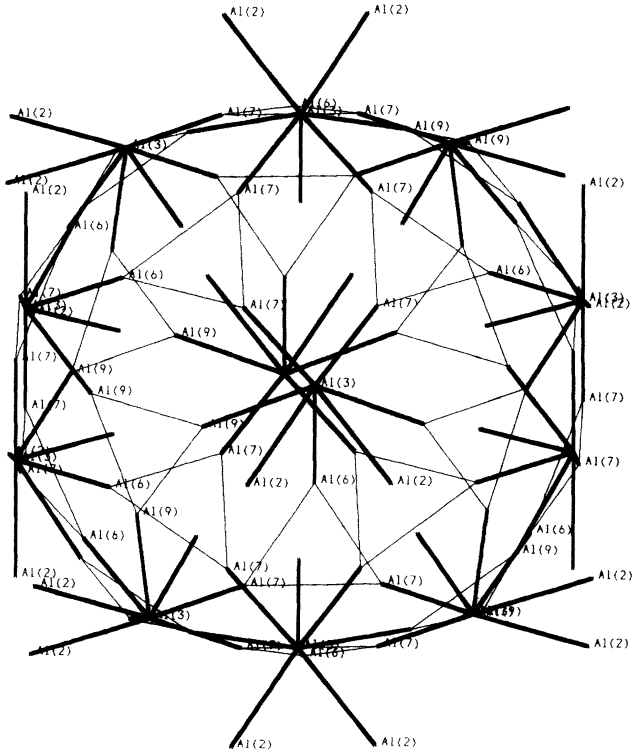

FIG. 4. Completed third shell, view near a pseudofivefold axis.

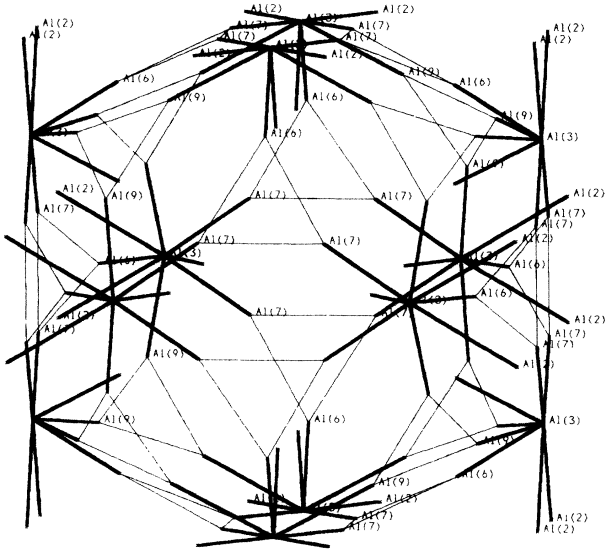

FIG. 5. Same, view near [001] axis.

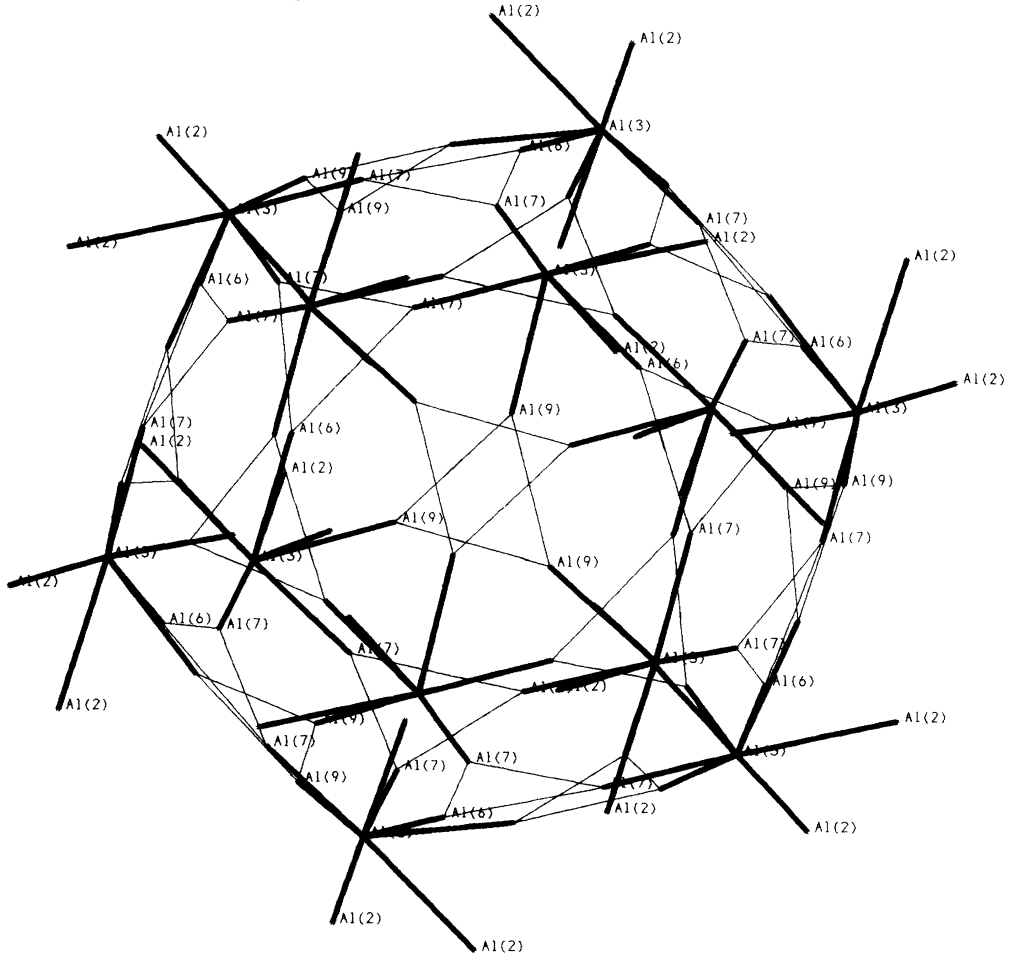

FIG. 6. Same, view near a [111] threefold axis.

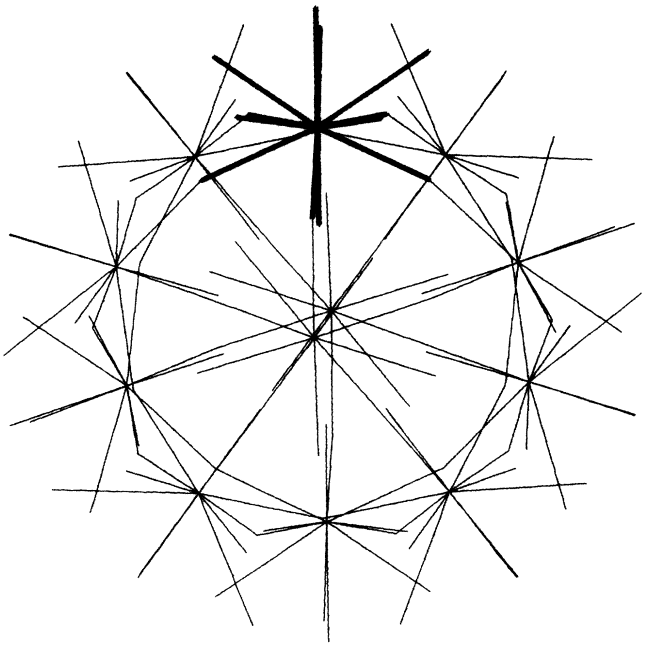

FIG. 7. The central triple shell of the α phase, simulated as an array of twelve icosahedral stars with shared Al(1) and Al(8) sites. View is near a pseudo-five-fold axis.

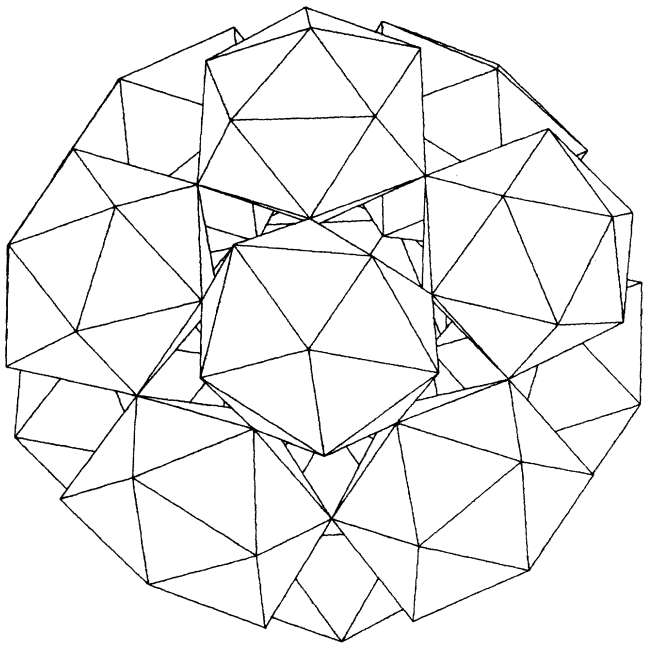

FIG. 8. The same, depicted as an array of opaque icosahedra (view angle is same as in Fig. 7.) The icosahedra make contact at the Al(1) and Al(8) sites, which have coordination number 12.

(i) It has 50 faces and 72 vertices, each vertex an occupied atomic site.

(ii) It has nearly perfect $(2,\bar{3},\bar{5})$ icosahedral rotation group symmetry, a higher symmetry than the operators used in the reconstruction.

(iii) It shares eight triangular faces [sites Al(9)] with second shells which surround the cube corners, and is slightly extended in these directions, as might be expected from the cubic bonding.

(iv) There are 20 triangular threefold faces [12 composed of Al(6) and Al(7) sites], representing truncations of a rhombic triacontahedron along threefold axes. There are 30 elongated hexagon faces normal to the twofold symmetry axes of the icosahedral system; eight of these lie in the faces of the unit cell, and are shared with neighboring cells. The resulting polyhedron is the dual of the acceptance-volume polyhedron postulated by Cahn and Gratias[15] for their parallel motif algorithm; theirs is a triacontahedron truncated along fivefold axes.

(v) The Al(3) sites, as may be seen from Fig. 2, have coordination 12 with bonds lying along the fivefold icosahedral-axis directions of the central systems.

An alternative treatment of the sites in the triple shell is to connect the same set of sites (generated as before, with only cubic symmetries) as a set of 12 icosahedral stars surrounding the Mn(1) sites, like the pattern suggested by Redfield and Zangwill.[10] This visualization is shown in Fig. 7, and again as a set of solid opaque icosahedral clusters in Fig. 8. Viewing the structure in this way makes clear the local-cluster topology of the triple shells. We note that the local icosahedral stars are not quite regular—see Table II for the neighbor-pair distances—Al(4) to Mn(1) and Mn(1) to Al(3) bonds are 20% shorter than the remaining bonds, and that the local fivefold symmetry axes of the small clusters are rotated 36° on the global fivefold axes of the MacKay shell, so that the Al(1) and Al(8) sites are shared between the local stars. In this grouping, the sites of the third shell in Figs. 4–6 are all outward-facing half-stars of the twelve icosahedral clusters on MacKay-icosahedron centers.

TABLE II. Neighbor-pair distances for the coordination icosahedron surrounding an Mn(1) site. Asterisk denotes errors in these estimates, from the least-squares fitting including Debye-Waller factors, on the order of ±1%. The errors on the remaining figures are less accurately confirmed.

Number of bonds	Type	Site numbers	Pair distance (Å)	
1	Radial from first shell	Al(4)-Mn(1)	2.405	*
3	Second (MacKay) shell	Mn(1)-Al(1)	2.544	*
2	Second-shell {111} triangle	Mn(1)-Al(8)	2.604	*
1	Radial to third shell	Mn(1)-Al(3)	2.460	*
2	Third-shell {111} triangle	Mn(1)-Al(9)	3.003	
2	Third shell	Mn(1)-Al(7)	2.802	
1	Third shell	Mn(1)-Al(6)	2.573	

TABLE III. Triple shells with cubic third-shell symmetry.

	α phases—$Pm\bar{3}$ Symmetry						
	Cooper (cell II) x-ray diffraction				Mozer and Cahn Corresponding corner shells moved to center of unit cell		
	x	y	z		x	y	z
Fe(1)	0.3243	0.1981	0.0000	Mn(1)	0.322 06	0.192 92	0.000 00
Fe(2)	0.1757	0.3019	0.5000	Mn(2)	0.171 24	0.302 46	0.500 00
Al(1)	0.3777	0.0000	0.0000		0.370 82	0.000 00	0.000 00
Al(2)	0.1223	0.5000	0.5000		0.132 82	0.500 00	0.500 00
Al(4)	0.1651	0.1006	0.0000		0.163 49	0.098 87	0.000 00
Al(5)	0.3349	0.3994	0.5000		0.335 35	0.398 66	0.500 00
Al(8)	0.1146	0.1872	0.3003		0.109 01	0.185 79	0.302 70
Al(9)	0.3854	0.3128	0.1997		0.382 47	0.312 50	0.200 66
Al(3)	0.2010	0.5000	0.0000		0.210 05	0.500 00	0.000 00
Al(6)	0.3725	0.3830	0.0000		0.377 04	0.380 73	0.000 00
Al(7)	0.1734	0.0970	0.5000		0.170 86	0.098 94	0.500 00

Thus the composite triple shell agrees in detail with the suggestion by Redfield and Zangwill, that icosahedral clusters of twelve aluminums around each Mn(1) site can be positioned (with a 36° axial rotation) to form the MacKay second-shell icosahedron, completely enclosed by a third shell of aluminums. We emphasize that all fivefold symmetries are intrinsic to the experimental data, and have not been introduced by the analysis method.

This high degree of ordering at the third-shell level has not been noted by previous authors. It is entirely consistent with the octahedral bonding pattern of manganese around threefold axes between MacKay double icosahedral clusters, which has been suggested[1,2,4] as an organizing principle for the icosahedral phase, and it adds considerable detail at the third-shell level.

A different consideration is also suggested by the $Pm\bar{3}$ structure of the α phase. Had we elected the corner of the unit cell to be at the center (an equivalent choice from the space-group information), and chosen to perform the reflection and inversion operations about that center, we would discover a third shell with a rotation group of lower symmetry [as we may already understand from the fact that Al(3) sites look different when viewed from the corner as center].

This situation was already anticipated in a paper by Cooper[16] describing the α phase of the (Al,Si)-Fe ternary compound. See the right-hand block of Table I, and the left-hand block of Table III. These list Cooper's "cell I" and "cell II" sites, which he describes as being arranged so that the phase appears like body-centered cubic, on the average.

The situation is illustrated in Fig. 9, where the two third shells are seen as they would appear to intersect on a $Pm\bar{3}$ lattice arrangement (this is primitive cubic, of lower symmetry than body centered). The inner shells only for each site, considered apart from the surrounding third shells, would appear to be in body-centered symmetry.

We see that the shell for cell II is nearly spherical in outline, containing a face pattern with nearly regular hexagons on twofold cubic axes, triangles on {111}-type axes (shared with the adjacent second shells), and irregular pentagons and triangles between. It is clear that the cell I shell can be identified with what we have already illustrated, and that Cooper is describing the $Pm\bar{3}$ geometry. Center and corner shell intersect along the ring of nine sites, which is illustrated in Figs. 3–5.

The large nearly regular hexagon which bisects the edge of the unit cell forms the center plane of a hexagonal bipyramid, whose end vertices—Al(2) sites in the MacKay shells of the corners—are separated by only 3.2 Å, too short an axis to permit an additional "interior" site. Thus the form of this shell indicates that the center-and-corner structure of Fig. 2 is space filling, in the Mn α phase as well as the Fe α phase; all plausible sphere sites have been shown.

Coordination-shell structures like those in Figs. 7 and 8, drawn around the Mn(2) sites, would have coordina-

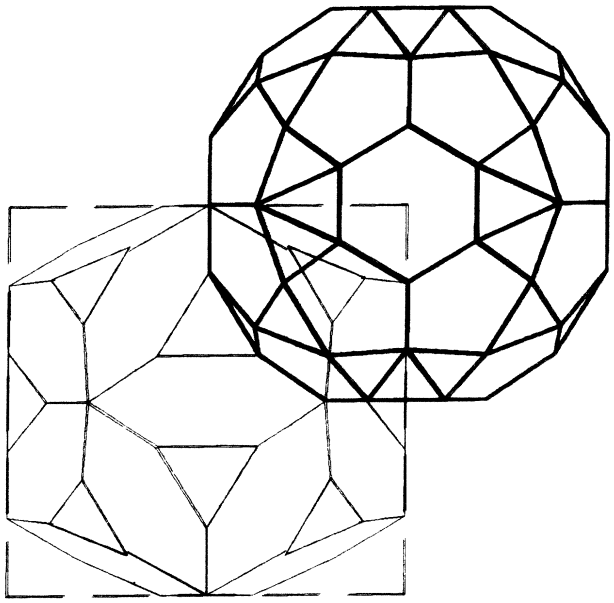

FIG. 9. Intersecting third shells—Cooper's cell I and cell II (emphasized).

tion 11 instead of 12, with irregular fivefold outward-facing half-stars.

SUMMARY

We find that the large third shell around hollow icosahedral centers may be visualized as a form having nearly perfect $(2,\bar{3},\bar{5})$ rotation group symmetry. Each triple shell shares triangular faces with double shells on the corners of the unit cell, and twofold extended-hexagon faces with adjacent unit cells. The third icosahedral shell makes good topological sense, fills all sites, and can be fitted consistently by the Redfield-Zangwill pattern of clustered icosahedral stars. Its form, combined with the complementary "corner" third shell, explains why only a $Pm\bar{3}$ space group is possible with this data set.

Note added. M. Audier has shown us his recent (unpublished) drawings of this phase, which closely resemble our Fig. 9.

ACKNOWLEDGMENTS

We are grateful to numerous colleagues for their contributions and encouragement. John Cahn provided the initial stimulus for this work, and has made many critically valuable suggestions. F. S. Biancanello and R. J. Schaefer furnished the careful specimen preparation. We have made extensive use of software routines developed by Stuart Cramer. Jesse Nunn wrote the large translator program CONVRT. Frederick C. Johnson has given consistent support for the project. Denis Gratias and Chris Henley have provided informative discussions.

[1]P. Guyot, M. Audier, and R. Lequette, *Proceedings of International Workshop on Aperiodic Crystals* [J. Phys. (Paris) Colloq. **C3**, 389 (1986)].

[2]M. Audier and P. Guyot, Ref. 1, p. 405.

[3]V. Elser, Phys. Rev. B **32**, 4892 (1985).

[4]V. Elser and C. L. Henley, Phys. Rev. Lett. **55**, 2883 (1985).

[5]C. L. Henley, Phys. Rev. B **34**, 797 (1986).

[6]D. Gratias, J. W. Cahn, W. Bessiere, Y. Calvayrac, S. Lefebvre, A. Quivy, and B. Mozer, in *New Theoretical Concepts in Physical Chemistry,* Proceedings of the NATO Advanced Research Workshop, Acquafredda di Maratea, Italy, 1987, edited by A. Amann, L. S. Cederbaum, and W. Gans (to be published). See also D. Gratias and J. Cahn, Scr. Metall. **20**, 1197 (1986), and C. Janot, J. Pannetier, M. de Boissieu, and J.-M. Dubois, Europhys. Lett. **3**, 995 (1987).

[7]M. Cornier, K. Zhang, R. Portier, and D. Gratias, J. Phys. (Paris) Colloq. **C3**, 447 (1986).

[8]L. Bendersky, J. Phys. (Paris) Colloq. **C3**, 457 (1986). See also L. Bendersky, J. Microsc. **146**, 303 (1987).

[9]A. L. MacKay, Acta Cryst. **15**, 916 (1962).

[10]A. C. Redfield and A. Zangwill, Phys. Rev. Lett. **58**, 2322 (1987).

[11]H. M. Rietveld, J. Appl. Cryst. **2**, 65 (1969).

[12]E. Prince, Nat. Bur. Stand. (U.S.) Misc. Publ. No. 1117, edited by F. J. Shorten (U.S. GPO, Washington, D.C., 1980), p. 8.

[13]M. Cooper and K. Robinson, Acta Cryst. **20**, 614 (1966).

[14]B. Mozer, J. Cahn, D. Gratias, and D. Shechtman, J. Phys. (Paris) Colloq. **C3**, 351 (1986).

[15]J. W. Cahn and D. Gratias, J. Phys. (Paris) Colloq. **C3**, 415 (1986).

[16]M. Cooper, Acta Cryst. **23**, 1106 (1967).